Active Site Structures and Catalytic Mechanism of *Rhodobacter sphaeroides* Dimethyl Sulfoxide Reductase as Revealed by Resonance Raman Spectroscopy

Shannon D. Garton,[†] James Hilton,[‡] Hiroyuki Oku,[†] Brian R. Crouse,[†] K. V. Rajagopalan,[‡] and Michael K. Johnson*,[†]

Contribution from the Department of Chemistry and Center for Metalloenzyme Studies, University of Georgia, Athens, Georgia 30602, and Department of Biochemistry, Duke University, Medical Center, Durham, North Carolina 27710

Received June 25, 1997. Revised Manuscript Received October 15, 1997[⊗]

Abstract: Resonance Raman spectra and excitation profiles (413−676 nm) are reported for four distinct forms of *Rhodobacter sphaeroides* dimethyl sulfoxide (DMSO) reductase: as prepared Mo(VI), dithionite-reduced Mo(IV), dimethyl sulfide reduced Mo(IV), and glycerol-inhibited Mo(V). All of the vibrational modes in the 200−1700 cm^{-1} region of the Mo(VI) and Mo(IV) forms are assigned to vibrations involving atoms in the first or second coordination sphere of the bis-molybdopterin-coordinated Mo active site, the dithiolene chelate rings, or nonresonantly enhanced protein modes. On the basis of $^{18}O/^{16}O$ isotope shifts, the Mo(VI) form is shown to be mono-oxo with ν(Mo═O) at 862 cm^{-1}, and the DMS-reduced Mo(IV) form is shown to involve bound DMSO with ν(Mo−O) at 497 cm^{-1} and ν(S═O) at 862 cm^{-1}. Bands at 536 and 513 cm^{-1} are tentatively assigned to ν(Mo−O(Ser)) stretching modes of coordinated serinate in the Mo(VI) and Mo(IV) forms, respectively. The vibrational modes of two distinct types of dithiolene chelate rings are identified on the basis of their excitation profiles, and the frequencies indicate that one is best viewed as a dithiolate ligand, while the other has more π-delocalized character. In the low-frequency region between 335 and 405 cm^{-1}, the Mo−S stretching modes of a distorted square pyramidal MoS_4 unit are assigned in each of the four derivatives investigated, based on the ^{34}S isotope shifts and sensitivity to Mo oxidation state. The average Mo−S bond strength increases with decreasing Mo oxidation state. Taken together, the Mo−S and dithiolene vibrational assignments indicate that all four of the molybdopterin dithiolene S atoms remain coordinated in each of the four forms investigated. Structures for each of these four derivatives are proposed on the basis of the resonance Raman results, and the ability to monitor directly the origin and fate of the Mo oxo group via isotopic labeling indicates that each corresponds to a catalytically competent intermediate in the reaction cycle. Overall, the results provide direct confirmation of an oxygen atom transfer mechanism, with the active site cycling between mono-oxo-Mo(VI) and des-oxo-Mo(IV) forms via a DMSO-bound Mo(IV) intermediate, and the molybdopterin dithiolene ligands staying firmly attached throughout the catalytic cycle.

Introduction

The recent proliferation of X-ray crystal structures for molybdenum-containing oxotransferases or hydroxylases has revealed considerable variability in the molybdenum active sites.[1−5] In all cases, molybdenum is coordinated by the dithiolene sides chains of one or two molybdopterins (see Figure 1), and in some cases, there are terminal oxo/sulfido ligands and protein side-chain ligands (serine, cysteine or selenocysteine). Moreover, recent crystallographic[3,4] and spectroscopic[6,7] data for two highly homologous dimethyl sulfoxide (DMSO) reductases from photosynthetic non-sulfur purple bacteria indicate that substantial flexibility in the Mo coordination environment can exist even within a specific enzyme or class of enzymes. Such structural flexibility leads to uncertainty in the catalytic mechanism, and the objectives of this study were to utilize resonance Raman spectroscopy both to define structures for the catalytically competent oxidized and reduced forms of DMSO reductase and to monitor directly the number, origin, and fate of molybdenum terminal oxo ligands.

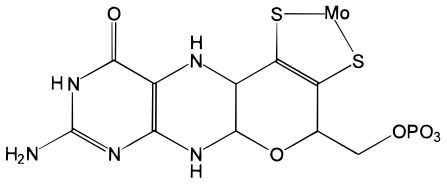

Figure 1. Structure of molybdopterin. The terminal phosphate is elaborated as a guanine dinucleotide in DMSO reductase.

The DMSO reductases from *Rhodobacter* species and biotin sulfoxide reductases from *Rhodobacter sphaeroides* and *Escherichia coli* are the only known molybdenum oxotransferases or hydroxylases to have the molybdenum cofactor center as their sole prosthetic group.[8,9] However, very different active-site structures have been reported for the oxidized (as prepared) forms of DMSO reductase from *R. sphaeroides*[3] and *Rhodo-*

[†] University of Georgia.
[‡] Duke University.
[⊗] Abstract published in *Advance ACS Abstracts,* December 15, 1997.

(1) Romao, M. J.; Archer, M.; Moura, I.; Moura, J. J. G.; LeGall, J.; Engh, R.; Schneider, M.; Hof, P.; Huber, R. *Science* **1995**, *270*, 1170−1176.
(2) Huber, R.; Hof, P.; Duarte, R. O.; Moura, J. J. G.; Moura, I.; Liu, M.-Y.; LeGall, J.; Hille, R.; Archer, M.; Romao, M. J. *Proc. Natl. Acad. Sci. U.S.A.* **1996**, *93*, 8846−8851.
(3) Schindelin, H.; Kisker, C.; Hilton, J.; Rajagopalan, K. V.; Rees, D. C. *Science* **1996**, *272*, 1616−1622.
(4) Schneider, F.; Löwe, J.; Huber, R.; Schindelin, H.; Kisker, C.; Knablein, J. *J. Mol. Biol.* **1996**, *263*, 53−69.
(5) Boyington, J. C.; Gladyshev, V. N.; Khangulov, S. V.; Stadtman, T.; Sun, P. D. *Science* **1997**, *275*, 1305−1308.
(6) Bennett, B.; Benson, N.; McEwan, A. G.; Bray, R. C. *Eur. J. Biochem.* **1994**, *225*, 321−331.
(7) George, G. N.; Hilton, J.; Rajagopalan, K. V. *J. Am. Chem. Soc.* **1996**, *118*, 1113−1117.

S0002-7863(97)02109-4 CCC: $14.00

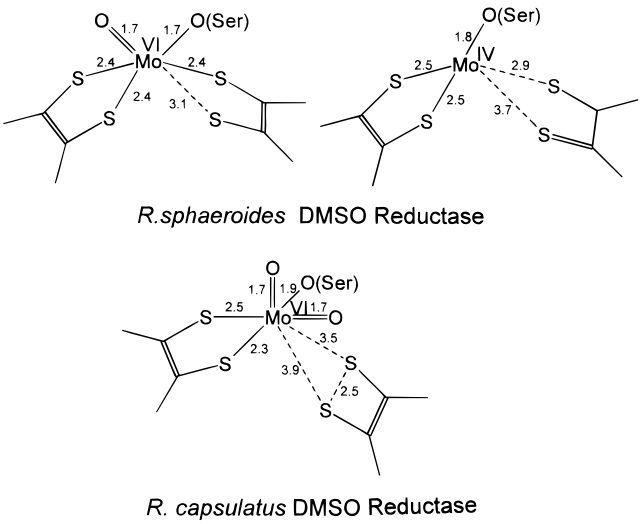

Figure 2. Active site structures of *R. sphaeroides* and *R. capsulatus* DMSO reductase as determined by X-ray crystallography.[3,4] Selected distances are given in angstroms.

bacter capsulatus[4] (see Figure 2). In *R. sphaeroides* DMSO reductase, the Mo(VI) site has a distorted trigonal prismatic geometry involving one symmetrically and one asymmetrically coordinated dithiolene, a single terminal oxo, and the oxygen of a deprotonated serine. Dithionite reduction in the crystalline state resulted in loss of the terminal oxo ligand and partial dissociation of one of the molybdopterin dithiolenes which appeared to have undergone a keto−enol tautomerization after protonation of the thiolate. This has led to a proposal of a direct oxotransferase mechanism involving the single oxo group with dithiolene dissociation on reduction facilitating substrate binding. Subsequent reassociation of the dithiolene was envisioned to trigger molybdenum oxidation, Mo═O bond formation, and product release.[3] In contrast, the Mo(VI) site in *R. capsulatus* DMSO reductase has square pyramidal geometry with two *cis*-oxo groups, one equatorial and one axial, with one of the molybdopterin dithiolenes and the serinate as the other equatorial ligands. The second molybdopterin is not part of the molybdenum coordination sphere and appears to have a weak S−S interaction.

Different active-site structures for the functional forms of these two enzymes are difficult to reconcile with the 80% sequence identity,[10] the almost superimposable protein structures,[3,4] and the close similarities in the absorption spectra of both the Mo(VI) and Mo(IV) forms[8,11,12] and the variable-temperature magnetic circular dichroism (VTMCD)[11,12] and EPR[6,8,11,12] properties of Mo(V) forms. However, the extensive EPR studies of Bray and co-workers on *R. capsulatus* DMSO reductase do indicate that different types of Mo(V) resonances are accessible depending on the nature of the reductant and/or the conditions of reduction.[6] The high-*g*-type EPR signals are indicative of a bis-dithiolene des-oxo-Mo(V) species[7] (presumably derived from reduction of bis-dithiolene, mono-oxo-Mo(VI) species, i.e., the *R. sphaeroides* structure[3]), whereas the low-*g*-type 1 EPR signal is indicative of a mono-oxo-Mo(V) species with a single dithiolene ligand[6] (presumably derived from reduction of a di-oxo-Mo(VI) species with a single dithiolene ligand, i.e., the *R. capsulatus* structure[4]). Hence, the differences in the Mo(VI) active structures for *R. capsulatus* and *R. sphaeroides* DMSO reductases most likely relate to crystallization conditions, but it is as yet unclear if either corresponds to the catalytically competent form of the enzyme in solution. Moreover, since dithionite reduction of *R. capsulatus* DMSO reductase can lead to either high-*g*- or low-*g*-type Mo(V) EPR signals (dependent on the nature of the buffering media), it is unclear if the structurally characterized dithionite-reduced form of *R. sphaeroides* DMSO reductase corresponds to a functional Mo(IV) species. In this connection, it is noteworthy that Mo-EXAFS studies on *R. sphaeroides* DMSO reductase are in reasonable agreement with the crystal structure in the Mo(VI) state but differ markedly for the Mo(IV) form.[7] In the Mo(VI) state, the first coordination sphere was shown to comprise one terminal oxo at 1.68 Å, approximately four thiolates at 2.44 Å, and one oxygen or nitrogen at 1.92 Å. EXAFS studies indicate des-oxo for the dithionite-reduced Mo(IV) state, but the dissociation of one of the dithiolenes to the extent seen in the crystal structure is not apparent. Best fits were obtained with three or four thiolates at 2.33 Å and two different oxygen or nitrogen ligands at 2.16 and 1.92 Å.

Resonance Raman studies of *R. sphaeroides* DMSO reductase provided the first direct evidence for molybdopterin coordination to Mo via the dithiolene unit.[13,14] Using red excitation (676 and 720 nm), Mo−S and C═C vibrations were observed in both the Mo(VI) and Mo(IV) states, and the former were assigned via $^{34}S/^{32}S$ isotope shifts. However, the vibrational assignments require reinterpretation in light of analytical[15] and crystallographic[3] evidence for two rather than one molybdopterin guanine dinucleotides at the active site. Moreover, no Mo═O vibrations were identified and high fluorescence backgrounds prevented the collection of spectra with higher energy excitation. Following our recent success in locating Mo═O and dithiolene stretching modes in the molybdenum domain of human sulfite oxidase,[16] we report here a detailed resonance Raman investigation of as prepared Mo(VI), glycerol-inhibited Mo(V), dithionite-reduced Mo(IV), and dimethyl sulfide (DMS) reduced Mo(IV) forms of *R. sphaeroides* DMSO reductase using excitation wavelengths in the range of 676−413 nm. For each derivative, all of the observed bands can be rationally assigned to vibrational modes involving the atoms in the first or second coordination sphere of molybdenum, the dithiolene chelate rings, or nonresonantly enhanced protein modes. Of particular importance are the identification, via $^{18}O/^{16}O$ isotope shifts, of a Mo═O stretching mode in the Mo(VI) state and the Mo−O and S═O stretching modes of bound DMSO in a DMS-reduced Mo(IV) form. The results provide direct confirmation of an oxotransferase mechanism,[17] with the active-site cycling between mono-oxo-Mo(VI) and des-oxo-Mo(IV) forms via a DMSO-bound Mo(IV) intermediate. Although different modes of binding are identified for each molybdopterin dithiolene ligands, both are shown to remain firmly attached during the catalytic cycle.

(8) (a) Bastian, N. R.; Kay, C. J.; Barber, M. J.; Rajagopalan, K. V. *J. Biol. Chem.* **1991**, *266*, 5−51. (b) McEwan, A. G.; Ferguson, S. J.; Jackson, J. B. *Biochem. J.* **1991**, *274*, 305−307.
(9) Pollock, V. V.; Barber, M. J. *J. Biol. Chem.* **1997**, *272*, 3355−3362.
(10) Knäblein, J.; Mann, K.; Ehlert, S.; Fonstein, M.; Huber, R.; Schneider, F. *J. Mol. Biol.* **1996**, *263*, 40−52.
(11) Finnegan, M. G.; Hilton, J.; Rajagopalan, K. V.; Johnson, M. K. *Inorg. Chem.* **1993**, *32*, 2616−2617.
(12) Benson, N.; Farrar, J. A.; McEwan, A. G.; Thomson, A. J. *FEBS Lett.* **1992**, *307*, 169−172.
(13) Gruber, S.; Kilpatrick, L.; Bastian, N. R.; Rajagopalan, K. V.; Spiro, T. G. *J. Am. Chem. Soc.* **1990**, *112*, 8179−8180.
(14) Kilpatrick, L.; Rajagopalan, K. V.; Hilton, J.; Bastian, N. R.; Stiefel, E. I.; Pilato, R. S.; Spiro, T. G. *Biochemistry* **1995**, *34*, 3032−3039.
(15) Hilton, J. C.; Rajagopalan, K. V. *Arch. Biochem. Biophys.* **1996**, *325*, 139−143.
(16) Garton, S. D.; Garrett, R. M.; Rajagopalan, K. V.; Johnson, M. K. *J. Am. Chem. Soc.* **1997**, *119*, 2590−2591.
(17) Schultz, B. E.; Hille, R.; Holm, R. H. *J. Am. Chem. Soc.* **1995**, *117*, 827−828.

Experimental Methods

Samples. *R. sphaeroides* DMSO reductase was purified and assayed as previously described.[8a,15] The samples used in this work had specific activities in the range of 15−20 μmol of DMSO reduced per minute per milligram of protein, equal or greater than the maximum reported values,[8a,15] and exhibited absorption characteristics identical to the published data.[6] Samples were prepared in a 50 mM tricine buffer, pH 7.5, and were concentrated to the range 2−4 mM for resonance Raman studies by centricon ultrafiltration. Exchange into the equivalent $H_2{}^{18}O$ buffer (prepared using $H_2{}^{18}O$ with 95−98% isotopic enrichment obtained from Cambridge Isotope Laboratories) was carried out by three 10-fold dilution and reconcentration cycles. Dithionite reduction was carried out anaerobically under argon in a Vacuum Atmospheres glovebox (<1 ppm O_2) by addition a single grain of solid dithionite. Reoxidation was accomplished by addition of DMSO or ferricyanide and excess oxidant was removed by at least two dilution/reconcentration cycles. ^{18}O-enriched DMSO ($DMS^{18}O$) was prepared by oxidation of DMS with Br_2 using pyridine as a base in 95% isotopically enriched $H_2{}^{18}O$ (obtained from CEA, Grenoble, France). The procedure followed the published protocol,[18] except that a slight excess of DMS was used rather than using $NaHSO_3$ to react with excess Br_2 in order to minimize $H_2{}^{16}O$ incorporation. The resulting sample was purified by vacuum distillation three times to remove fluorescent impurities, and EI-MS analysis using a Finnigan-4000 GC/MS indicated 95% isotopic enrichment for $DMS^{18}O$. DMS-reduced samples were obtained by addition of a 20-fold stoichiometric excess of DMS. The glycerol-inhibited Mo(V) sample was prepared as previously described,[11] by reduction with a stoichiometric amount of reduced benzyl viologen followed by the addition of 50% (v/v) glycerol. Once prepared this derivative is insensitive to O_2 or repeated freezing/thawing, and excess glycerol was removed prior to resonance Raman studies by successive dilution and reconcentration cycles.

Spectroscopic Methods. UV−vis absorption spectra were recorded under anaerobic conditions in septum-sealed 1 mm cuvettes using a Shimadzu UV-3101PC spectrophotometer. X-Band (~9.5 GHz) EPR spectra were recorded on a Bruker ESP-300E EPR spectrometer equipped with a ER-4116 dual mode cavity and an Oxford Instruments ESR-9 flow cryostat. Spin quantitations were carried out under nonsaturating conditions using 1 mM CuEDTA as the standard.

Resonance Raman spectra were recorded using an Instruments SA Ramanor U1000 spectrometer fitted with a cooled RCA 31034 photomultiplier tube with 90° scattering geometry. Spectra were recorded digitally using photon counting electronics, and improvements in signal-to-noise were achieved by signal averaging multiple scans. Band positions were calibrated using the excitation frequency and CCl_4 and are accurate to ± 1 cm^{-1}. Lines from a Coherent Innova 100 10-W argon ion laser or Coherent Innova 200-K2 krypton ion laser were used for excitation, and plasma lines were removed using a Pellin Broca Prism premonochromator. Scattering was collected from the surface of a frozen 10 μL droplet of sample using a custom-designed anaerobic sample cell,[19] attached to the cold finger of an Air Products Displex Model CSA-202E closed cycle refrigerator. This arrangement enables samples to be cooled down to 25 K, which facilitates improved spectral resolution and prevents laser-induced sample degradation. The high fluorescence backgrounds exhibited by some DMSO reductase samples using visible excitation were minimized by exposing the frozen samples to the laser beam for at least 6 h prior to data collection. We attribute this phenomena to quenching of the fluorescence from an unidentified impurity (probably via gradual population of triplet state under conditions of continuous illumination at low temperature), since the fluorescence intensity was variable for different preparations. However, the observed Raman bands were apparent prior to prolonged laser exposure, albeit with lower signal-to-noise, and no new Raman bands appeared as the background fluorescence decreased. The ice band at 231 cm^{-1} or the 679 cm^{-1} band of residual DMSO in DMSO-reoxidized samples was used as the internal standards for excitation profiles.

(18) Okrusek, A. *J. Labelled Compd. Radiopharm.* **1983**, *20*, 741−743.
(19) Drozdzewski, P. M.; Johnson, M. K. *Appl. Spectrosc.* **1988**, *42*, 1575−1577.

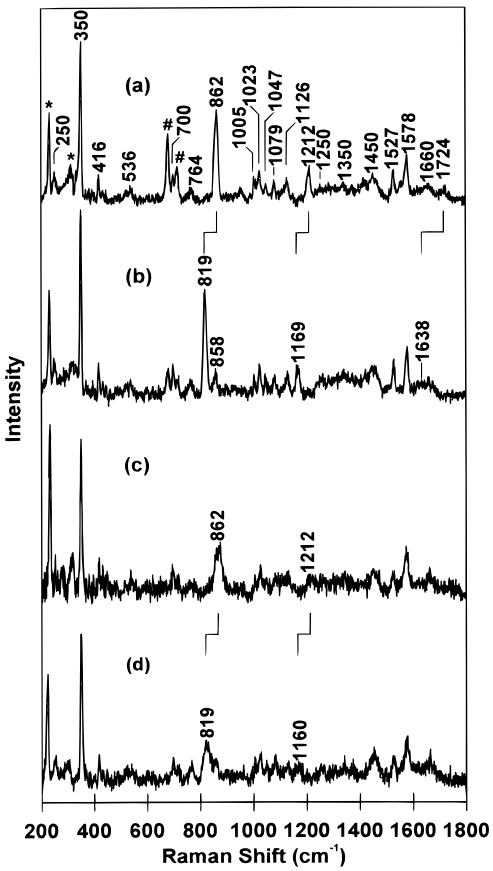

Figure 3. Resonance Raman spectra of Mo(VI) forms of DMSO reductase with 568 nm excitation. (a) Dithionite-reduced and reoxidized with $DMS^{16}O$; (b) dithionite-reduced and reoxidized with $DMS^{18}O$; (c) as prepared; (d) exchanged into $H_2{}^{18}O$ buffer, dithionite-reduced, and ferricyanide-oxidized. The spectra were obtained with samples (2−6 mM in DMSO reductase) frozen at 25 K, using 70−95 mW incident laser power and 6.5 cm^{-1} spectral resolution, and are the sum of 20, 20, 25, and 25 scans for a, b, c, and d, respectively. Each scan involved photon counting for 1 s every 1 cm^{-1}. A linear ramp fluorescent background has been subtracted from each spectrum. The lattice modes of ice at 231 and 310 cm^{-1} which shift to 221 and 300 cm^{-1} for the sample in $H_2{}^{18}O$ buffer (d) are marked by an asterisk. The vibrational modes of residual DMSO that was not completely removed by centricon dialysis are marked by a pound sign (#).

Results

Four spectroscopically distinct forms of *R. sphaeroides* DMSO reductase were investigated by resonance Raman using excitation wavelengths in the range of 413−676 nm: as-prepared or re-oxidized Mo(VI) (Figures 3, 4, and 8); dithionite-reduced Mo(IV) (Figures 5, 7, and 8); DMS-reduced Mo(IV) (Figure 6, 7, and 8); glycerol-inhibited Mo(V) (Figure 8). Resonance Raman spectra for the Mo(VI), dithionite-reduced Mo(IV) and DMS-reduced Mo(IV) forms are shown in the range of 200−1800 cm^{-1} (Figures 3, 4, 6 and 8), and complete vibrational assignments are tabulated in Table 1. For the glycerol-inhibited Mo(V) species, resonance Raman data (Figure 8) and assignments (Table 1) are limited to the 200−550 cm^{-1} region, since data collection and detailed analysis of the complex high-frequency region using isotopically labeled glycerol are still in progress. On the basis of EPR spin quantitations, the glycerol-inhibited Mo(V) species was assessed as being trapped exclusively in the Mo(V) state, unsplit $g = 1.99, 1.98, 1.96$ resonance accounting for 0.95 ± 0.10 spins/Mo.[11] Each of the four species investigated in this work has a distinctive absorption spectrum, and the samples of as-prepared Mo(VI), glycerol-inhibited Mo(V), and dithionite-reduced Mo(IV) used for

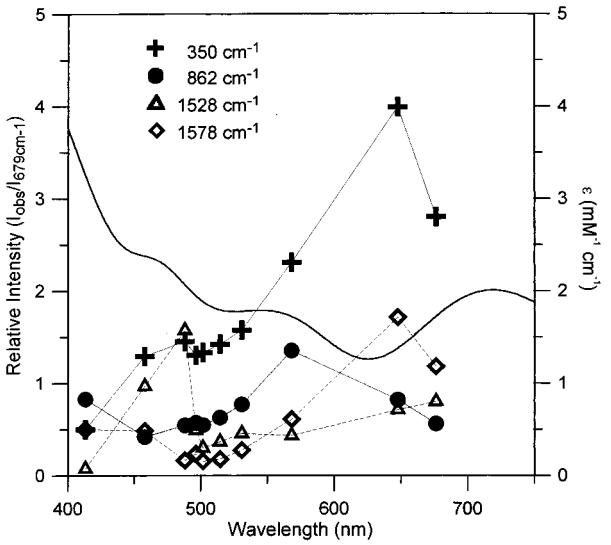

Figure 4. Absorption spectrum and excitation profiles for Mo(VI) DMSO reductase. The sample used for the resonance Raman studies is the same as in Figure 3a. The intensities of the bands at 350, 862, 1527, and 1578 cm^{-1} were normalized to that of the nonresonantly enhanced DMSO band at 679 cm^{-1} which acted as the internal standard.

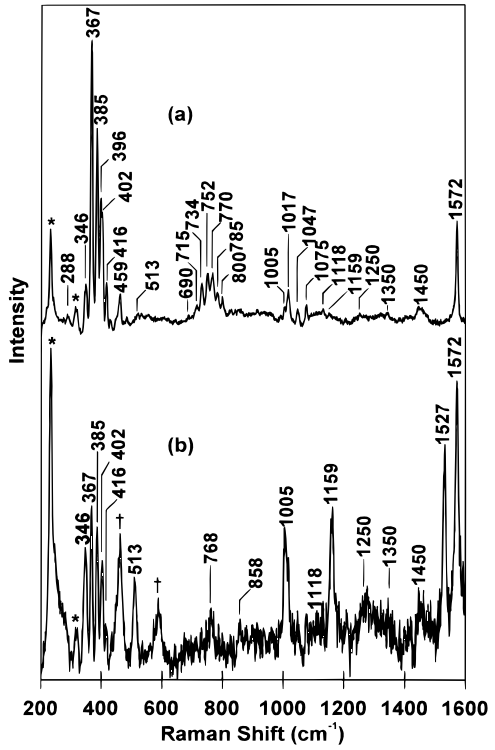

Figure 5. Resonance Raman spectra of dithionite-reduced Mo(IV) DMSO reductase. (a) Dithionite-reduced DMSO reductase (∼2 mM) with 568 nm excitation; sum of 25 scans. (b) Dithionite-reduced DMSO reductase (∼3 mM) with 488 nm excitation; sum of 12 scans. The bands at 461 and 589 cm^{-1} (marked by †) arise from excess dithionite.[33] All other data collection and handling procedures are as described in Figure 3.

resonance Raman studies exhibited spectra identical with the published data.[8a,11] The spectroscopic consequences of DMS reduction have not been reported previously, but it was immediately apparent from visual inspection that the reduced sample obtained with DMS (cherry red) was quite distinct from that produced by dithionite (lime green). The absorption spectra of these two Mo(IV) forms are shown in Figure 7, along with excitation profiles for selected resonance Raman bands.

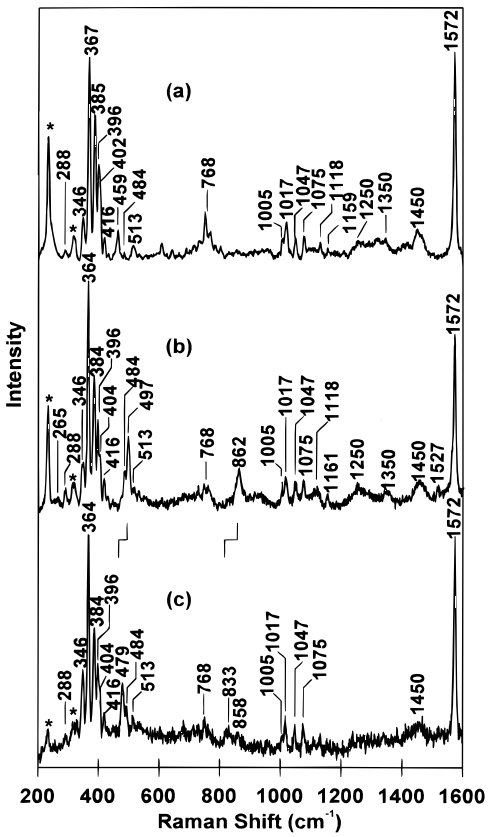

Figure 6. Resonance Raman spectra of dithionite-reduced and DMS-reduced Mo(IV) DMSO reductase with 530 nm excitation. (a) Dithionite-reduced DMSO reductase in $H_2{}^{16}O$ buffer (the same sample as used in Figure 5a); (b) DMS-reduced DMSO reductase (∼2 mM); (c) DMS-reduced DMSO reductase sample (∼6 mM) that had been dithionite-reduced and reoxidized with $DMS^{18}O$ (∼4 mM). The data collection and handling procedures are as described in Figure 3. Spectra a, b, and c are the sum of 25, 13, and 15 scans, respectively.

Since many of the vibrational modes observed are common to all four forms of DMSO reductase investigated, the assignments presented in Table 1 are rationalized below, delineated in terms of vibrational mode rather than different forms of DMSO reductase. All of the observed bands in each resonance Raman spectrum can be rationally assigned to Mo═O, Mo−O(Ser), Mo−S(dithiolene), Mo−O, and S═O of bound DMSO, or dithiolene vibrational modes with the exception of weak broad bands centered at 1250, 1350, 1450, and 1660 cm^{-1}. These bands are characteristic of the most intense nonresonantly enhanced Raman bands of polypeptides[20] and are assigned to amide III (1250 cm^{-1}), tryptophan (1350 cm^{-1}), CH_2 bending (1450 cm^{-1}), and amide I (1660 cm^{-1}).

Mo═O Stretching Mode. As-prepared and reoxidized Mo(VI) samples of DMSO reductase have an intense band at 862 cm^{-1} that dominates the mid-frequency region of the resonance Raman spectrum with 568 nm excitation (see Figure 3). The band sharpens appreciably on dithionite reduction followed by reoxidation with substrate, DMSO, suggesting heterogeneity in the enzyme as prepared. Unambiguous assignment of this band to a Mo═O stretching mode of a *single* terminal oxo group is based on the loss of this band on dithionite reduction (see Figure 5) and the 43 cm^{-1} downshift that is observed for samples reoxidized with ferricyanide after exchange into $H_2{}^{18}O$ buffer or using $DMS^{18}O$ (see Figure 3). These isotope shifts were not observed in control experiments in which dithionite-reduced samples were reoxidized after equivalent

(20) Fabian, H.; Anzenbacher, P. *Vib. Spectrosc.* **1993**, *4*, 125−148.

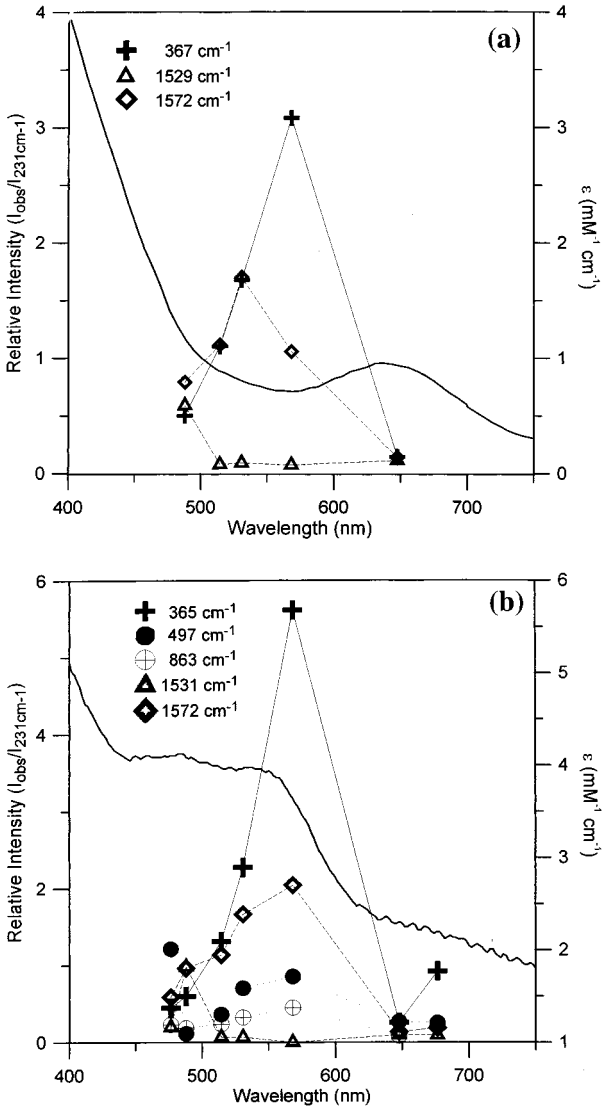

Figure 7. Absorption spectra and excitation profiles for dithionite-reduced and DMS-reduced Mo(IV) DMSO reductase: (a) dithionite-reduced DMSO reductase (the same sample as that used in Figure 5c); (b) DMS-reduced DMSO reductase (the same sample as that used in Figure 6b). The intensities of the Raman bands were normalized to that of the nonresonantly enhanced ice-band at 231 cm^{-1} which acted as the internal standard.

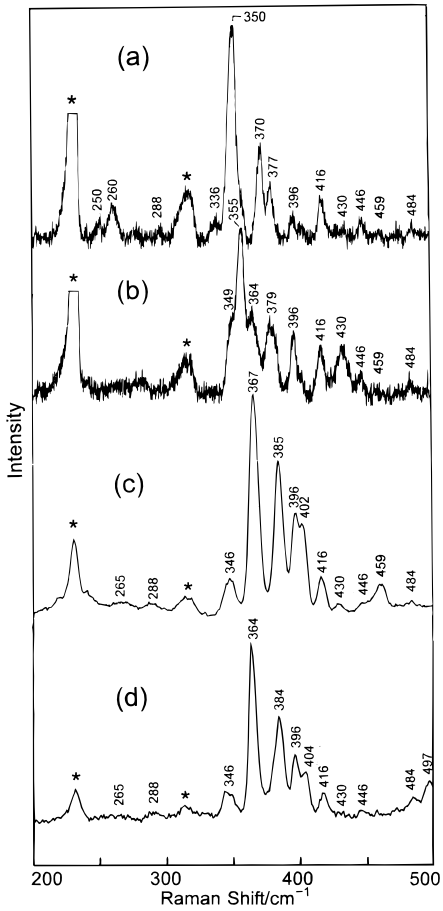

Figure 8. Resonance Raman spectra in the Mo−S stretching region for Mo(VI), Mo(V), and Mo(IV) DMSO reductase samples: (a) as-prepared Mo(VI) DMSO reductase (∼3 mM) with 676 nm excitation; (b) glycerol-inhibited Mo(V) DMSO reductase (∼2 mM) with 676 nm excitation after removal of excess glycerol; (c) dithionite-reduced Mo-(IV) DMSO reductase with 568 nm excitation (low-frequency region of spectrum shown in Figure 5a); (d) DMS-reduced Mo(IV) DMSO reductase with 568 nm excitation (the same sample as that used in Figure 6b). Spectra a and b involved photon counting for 1 s every 0.2 cm^{-1}. All other data collection and handling procedures are as described in Figure 3. Spectra a, b, c and d are the sum of 45, 50, 25, and 25 scans, respectively.

exchange with a $H_2{}^{16}O$ buffer or with $DMS^{16}O$. A 42 cm^{-1} ^{18}O downshift in the fundamental is predicted purely on the basis of mass effect for a Mo═O vibration at 862 cm^{-1}. As recently shown for sulfite oxidase, symmetric and asymmetric MoO_2 stretching modes each with a substantially smaller ^{18}O isotope shift (<33 cm^{-1}) would be expected for a *cis*-MoO_2 center with only one exchangeable oxo group.[16] While the band that remains at 862 cm^{-1} in the $H_2{}^{18}O$-exchanged sample is due to incomplete buffer exchange, the band that remains at 858 cm^{-1} in the $DMS^{18}O$-reoxidized sample is unlikely to result from residual Mo═^{16}O. Spectral overlays clearly show that the band is shifted in frequency and the intensity is at least twice that anticipated on the basis of the 95% enrichment of the $DMS^{18}O$ established by mass spectrometry. As discussed below, the underlying band at 858 cm^{-1} is attributed to the C−S stretching mode of one of the coordinated dithiolenes.

The excitation profile data in Figure 4 show that the Mo═O stretching mode at 862 cm^{-1} is maximally enhanced with 568 nm excitation. In the DMSO-reoxidized samples, the intensity of this band at this excitation wavelength permits observation of the first overtone at 1724 cm^{-1} (identified by a 86-cm^{-1} ^{18}O downshift in the ^{18}O minus ^{16}O difference spectrum) and a ν_s-$(A_1)(MoS_4)$ + ν(Mo═O) combination band at 1212 cm^{-1} (identified by a 43 cm^{-1} ^{18}O downshift). In contrast, the stretching modes of one type of dithiolene and Mo−S are maximally enhanced with 646 nm excitation, while the other type of dithiolene has stretching modes that receive maximum enhancement at 488 nm. Therefore, it seems likely that an oxo-to-Mo(VI) charge transfer transition is responsible for the resonance enhancement and at least in part for the absorption band centered at 560 nm.

Dithiolene Vibrational Modes. A graphical description of the five distinct types of molybdopterin dithiolene stretching modes associated with the *cis*-$C_2C_2S_2$ unit under local C_{2v} symmetry are shown in Figure 9. Estimates of the anticipated frequency ranges for each of these modes can be made on the basis of the detailed vibrational analysis of transition metal dithiolene complexes containing the equivalent unit, e.g., $[Ni(S_2C_2(CN)_2)_2]^{2-,-}$ [21] and $[M(S_2C_2(CN)_2)_3]^{2-}$ (M = V, Mo, W):[22] ν(C−S), 760−900 cm^{-1}; ν(C−C), ν(C−C) + ν(C−S), and ν-

(21) Schläpfer, C. W.; Nakamoto, K. *Inorg. Chem.* **1975**, *14*, 1338−1344.

Table 1. Vibrational Assignments (cm^{-1}) for DMSO-Oxidized (Mo(VI)), Glycerol-Inhibited (Mo(V)), Dithionite-Reduced (Mo(IV)), and DMS-Reduced (DMSO-Bound Mo(IV)) Forms of DMSO Reductase[a]

assignment[b]	Mo(VI)	Mo(V)	Mo(IV)	DMSO-bound Mo(IV)
π_d(E)(MoS_4)	250(1)		265	265
	260(2)			
dithiolene ring def.	288		288	288
$\nu_a(B_1)$(MoS_4)	336(3)	349	346(7)	346
$\nu_s(A_1)$(MoS_4)	350(7)	355	367(6)	364
ν_d(E)(MoS_4)	370(4)	364	385(4)	384
	377(3)	379	402	404
dithiolene or pyran ring deformations	396(1)	396	396(2)	396
	416(0)	416	416	416
	430	430	430(2)	430
	446	446	446	446
	459	459	459	
	484	484	484	484
ν(Mo−O) (bound DMSO)				497(18)
ν(Mo−O(Ser))	536		513	513
$2 \times \nu_a(B_1)$(MoS_4)			690	690
$[\nu_a(B_1) + \nu_s(A_1)]$($MoS_4$)			715	710
$2 \times \nu_s(A_1)$(MoS_4)	700		734	728
$[\nu_s(A_1) + \nu_d(E_a)]$($MoS_4$)			752	747
dithiolene(1) ν(C−S)	764		768	768
$2 \times \nu_d(E_a)$(MoS_4)			770	766
$[\nu_d(E_a) + \nu_d(E_b)]$($MoS_4$)			785	787
$2 \times \nu_d(E_b)$(MoS_4)			800	808
dithiolene(2) ν(C−S)	858		858	858
ν(Mo═O)	862(43)			
ν(S═O) (bound DMSO)				862(29)
dithiolene(2) ν(C−C)	1005		1005	1005
dithiolene(1) ν(C−C)	1023		1017	1017
dithiolene(1) ν(C−S) + ν(C−C)	1047		1047	1047
dithiolene(1) ν(C−C) + ν(C−S)	1079		1075	1075
dithiolene(2) ν(C−S) + ν(C−C)	1126		1118	1118
dithiolene(2) ν(C−C) + ν(C−S)	1160		1159	1161
$\nu_s(A_1)$(MoS_4) + ν(Mo═O)	1212(43)			
protein, amide III	1250		1250	1250
protein, tryptophan	1350		1350	1350
protein, $\delta(CH_2)$	1450		1450	1450
dithiolene(2) ν(C═C)	1527		1527	1527
dithiolene(1) ν(C═C)	1578		1572	1572
protein, amide I	1660		1660	1660
$2 \times \nu$(Mo═O)	1724(86)			

[a] Numbers in parentheses are ^{34}S or ^{18}O isotope shifts as dictated by the vibrational assignment. The ^{34}S isotope shifts are taken from Kilpatrick et al.[14] [b] Modes of the square pyramidal MoS_4 unit are assigned under idealized C_{4v} symmetry. The E-modes are expected to split for two bidentate dithiolene ligands (labeled E_a and E_b in overtone and combination band analysis).

(C−S) + ν(C−C) all in the region 1000−1180 cm^{-1}; ν(C═C) in the range of 1400−1600 cm^{-1}. Within these ranges, the ν-(C−S) and ν(C═C) frequencies are inversely correlated with low ν(C−S) and high ν(C═C) indicating that the dithiolene is effectively acting as a dithiolate ligand, whereas high ν(C−S) and low ν(C═C) indicates substantial π-delocalization and some dithioketone character, i.e. intermediate between the formal oxidized and reduced forms of the ligand:

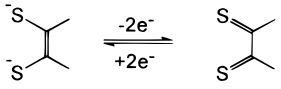

Two distinct types of coordinated dithiolene that are readily differentiated on the basis of their markedly different excitation profiles (Figures 4 and 7) are observed in the resonance Raman spectra of both Mo(VI) and Mo(IV) samples of DMSO reductase

(22) Clark, R. J. H.; Turtle, P. C. *J. Chem. Soc., Dalton Trans.* **1978**, 1714−1721.

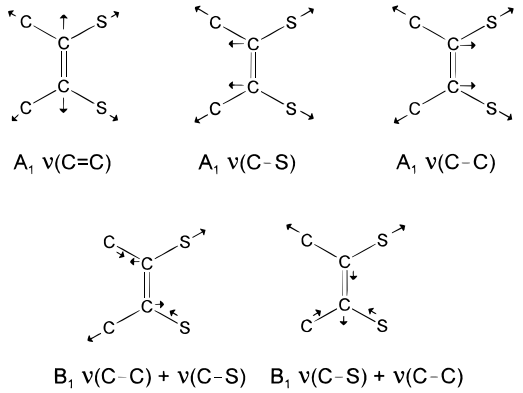

Figure 9. Schematic depiction of the vibrational modes of a *cis*-$C_2C_2S_2$ dithiolene unit under C_{2v} symmetry.

(see Table 1). In both oxidation states, dithiolene(1) stretching modes are maximally enhanced with low-energy excitation (excitation profile maxima near 646 and 530 nm for the Mo(VI) and Mo(IV) forms, respectively, see Figures 4 and 7) and are assigned to bands at 764−768 cm^{-1} (ν(C−S)), 1017−1023 cm^{-1} (ν(C−C)), 1047 cm^{-1} (ν(C−S) + ν(C−C)), 1075−1079 cm^{-1} (ν(C−C) + ν(C−S)), and 1572−1578 cm^{-1} (ν(C═C)) (see Figures 3, 5, and 6). In the Mo(IV) states with 568 nm excitation, the 768 cm^{-1} band is obscured by intense overtones and combination bands of MoS_4 stretching modes (Figure 5a) but is clearly observed with 488 nm (Figure 5b) and 530 nm (Figure 6a) excitation when the MoS_4 stretching modes are less strongly enhanced. The 568 nm spectrum of the dithionite-reduced Mo(IV) form (Figure 5a) is particularly useful for identifying the remaining stretching modes of dithiolene(1), since dithiolene(2) modes are only very weakly enhanced at this wavelength in Mo(IV) samples. The observed ν(C−S) and ν(C═C) stretching frequencies of dithiolene(1) are characteristic of single and double bonds, respectively, indicating that it is best viewed as a coordinated dithiolate.

The dithiolene(2) stretching modes are remarkably insensitive to the Mo oxidation state and are maximally enhanced with 488 nm excitation in both Mo(IV) and Mo(VI) oxidation states (Figures 4 and 7). Bands at 858, 1005, 1118−1126, 1159−1161, and 1527 cm^{-1} are assigned to ν(C−S), ν(C−C), ν(C−S) + ν(C−C), ν(C−C) + ν(C−S), and ν(C═C), respectively (see Figures 3, 5, and 6), and the frequencies are indicative of a more π-delocalized dithiolene ligand. In Mo(VI) samples, these bands are only clearly observed with excitation wavelengths <500 nm, with maximal enhancement with 488 nm excitation (data not shown), and the 1160 cm^{-1} band, in particular, is not significantly enhanced with 568 nm excitation (Figure 3). Figure 5b illustrates the dramatic enhancement of the dithiolene(2) modes that occurs with 488 nm excitation in Mo(IV) samples. The weak C−S stretching band of dithiolene-(2) at 858 cm^{-1} is obscured by the Mo═O stretching band in natural abundance Mo(VI) samples (862 cm^{-1}) and the S═O stretching mode of bound DMSO in the natural abundance DMS-reduced Mo(IV) sample (862 cm^{-1}, see below) but is apparent in the equivalent ^{18}O-labeled samples (Figures 3b and 6c) and in dithionite-reduced Mo(IV) samples using 488 nm excitation (Figure 5b). A similar set of bands with analogous relative intensities and excitation dependence was observed in the oxidized molybdenum domain of human sulfite oxidase: ν-(C−S) at 864 cm^{-1}, ν(C−C) at 1006 cm^{-1}, ν(C−S) + ν(C−C) at 1093 cm^{-1} (observed but not assigned in published data), ν(C−C) + ν(C−S) at 1161 cm^{-1}, and ν(C═C) at 1532 cm^{-1}.[16] Hence, this type of π-delocalized dithiolene appears to be common to both DMSO reductase and sulfite oxidase.

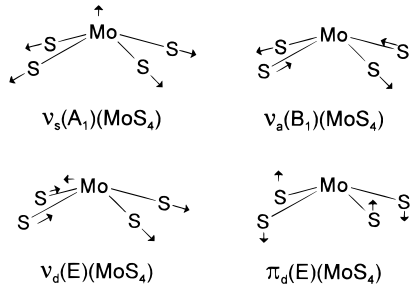

Figure 10. Schematic depiction of the vibrational modes of a square pyramidal (C_{4v}) MoS_4 unit expected at frequencies >200 cm^{-1}.

While the assignments of the ν(C−S) and ν(C═C) modes for each type of dithiolene are dictated by the vibrational analysis of transition metal dithiolene complexes, the rationale behind the assignment of the other three stretching modes requires some explanation. The ν(C−C) mode assignment is based on the expectation that it will be least sensitive of all five stretching modes to the extent of π-delocalization in the dithiolene chelate ring. The remaining two modes both involve a contribution from C−S stretching and hence are expected to occur at substantially higher frequencies in the π-delocalized dithiolene. The assignments of the ν(C−S) + ν(C−C) and ν(C−C) + ν-(C−S) modes depicted in Figure 9 are based on normal mode calculations for transition metal dithiolene complexes, which place the latter mode higher in energy.[21]

There are several bands in the low-frequency region that are good candidates for dithiolene or possibly pyran ring deformations. As discussed below, the Mo-S stretching modes can be identified on the basis of published ^{34}S isotope shifts and their sensitivity to the Mo oxidation state. Dithiolene ring deformation might also be expected to exhibit ^{34}S isotope shifts, but they are expected to be insensitive to $H_2{}^{18}O$ exchange and relatively invariant to Mo oxidation state given the insensitivity of the C−C, C−S, and C═C stretching modes to changes in the Mo oxidation state. On the basis of these criteria, the weak bands at 396, 416, 430, 446, 461, and 484 cm^{-1} that are observed in the low-frequency region of Mo(VI), Mo(V), and Mo(IV) forms (Figure 8) are tentatively assigned to dithiolene or pyran ring deformations (Table 1).

Mo−O(Ser) Stretching Mode. The bands at 536 cm^{-1} in the Mo(VI) samples (Figure 3) and at 513 cm^{-1} in the Mo(IV) samples (Figures 5 and 6) are assigned to Mo−O(Ser) stretching modes. The rationale for this assignment is the marked sensitivity to Mo oxidation state, the insensitivity to $H_2{}^{18}O$ exchange, and the loss of bands in this region in the glycerol-inhibited Mo(V) species (data not shown), in which the serinate and hydroxide ligands are believed to be replaced by a bidentate diol.[7,11,23] While this assignment should be viewed as tentative in the absence of isotopic labeling or site-directed mutagenesis studies, it is consistent with serinate ligation being maintained throughout the catalytic cycle.

Mo−S Stretching Modes. The four stretching modes of a square pyramidal MoS_4 unit under idealized C_{4v} symmetry are depicted in Figure 10, along with the only deformation mode expected to occur above 200 cm^{-1}.[24] Although detailed analyses of the vibrational modes of a square pyramidal MoS_4 are not available, a good indication of the relative frequencies expected for these modes is provided by square pyramidal Mo complexes such as $[MoOCl_4]^-$: $\pi_d(E)(MoCl_4)$, 240 cm^{-1}; $\nu_a(B_1)(MoCl_4)$, 327 cm^{-1}; $\nu_s(A_1)(MoCl_4)$, 354 cm^{-1}; $\nu_d(E)(MoCl_4)$, 364 cm^{-1}.[24,25] The same overall pattern is expected for the MoS_4 unit in DMSO reductase, but with split E-modes due to the bidentate dithiolenes. With this in mind, the criteria used for assigning Mo−S vibrational modes were sensitivity to Mo oxidation state and the ^{34}S isotope shift data published by Spiro and co-workers.[13,14]

Resonance Raman spectra in the Mo−S stretching region for all four of the DMSO reductase derivatives investigated in this work are shown in Figure 8. In each case, the symmetric breathing mode, $\nu_s(A_1)(MoS_4)$, which occurs at 350, 355, 367, and 364 cm^{-1} for the Mo(IV), Mo(V), dithionite-reduced Mo-(IV), and DMS-reduced Mo(IV) forms, respectively, is the most intense band at all wavelengths and is flanked by the lower energy $\nu_a(B_1)(MoS_4)$ mode and the two components of the higher energy $\nu_d(E)(MoS_4)$ mode. These asymmetric MoS_4 stretching modes are assigned based on their sensitivity to the Mo oxidation state, and all four Mo−S stretching modes show ^{34}S isotope shifts of 3−7 cm^{-1}, in the cases for which this data is available (see Table 1). The maximum theoretical isotope shift is ∼8 cm^{-1}, and values approaching this are only expected for the symmetric breathing mode. This reassignment of the Mo−S stretching modes provides further evidence that all four dithiolene S atoms remain firmly attached to Mo in all of the forms investigated in this work. Indeed, the overall increase in frequency with decreasing oxidation state indicates stronger rather than weaker Mo−S bonds, on average, on reduction to the catalytically competent Mo(IV) states. Since analogous behavior is observed for the bands in the 250−265 region, these are tentatively assigned to the components of the $\pi_d(E)(MoS_4)$ deformation mode.

The Mo(VI) spectrum with 676 nm excitation is in excellent agreement with the previously published spectrum[13,14] and the excitation profile for the symmetric breathing mode at 350 cm^{-1} indicates maximal enhancement under the low-energy dithiolate-to-Mo(VI) charge transfer band at 720 nm (Figure 4). The dithionite-reduced Mo(IV) spectrum obtained in this work with 676 nm excitation (data not shown) is similar to the published spectrum,[14] except for differences of up to 4 cm^{-1} in some of the band positions. However, the excitation profile for the symmetric breathing mode indicates maximal enhancement near 568 nm (Figure 7), and Mo(IV) spectra with dramatically improved signal-to-noise compared to the published data were obtained with 568, 530, and 488 nm excitation. The spectra at each of these wavelengths are dominated by four bands at 346, 367, 385, and 402 cm^{-1} (Figures 5, 6, and 8), which are assigned to the Mo−S stretching modes. This assignment is supported by ^{34}S isotope shifts for the 346, 367, and 385 cm^{-1} bands (7, 6 and 4 cm^{-1}, respectively). Unfortunately ^{34}S-isotope shift data are not available for the 402-cm^{-1}, since it is obscured by the dithiolene ring deformation modes at 396 cm^{-1} in the published data obtained with 676 nm excitation. Very similar bands with analogous excitation profiles (Figure 7) and small, but reproducible, shifts in the Mo−S stretching frequencies were observed in the DMS-reduced sample (Figures 6−8). This is in accord with a Mo(IV) species and indicates that only minor changes in dithiolene ligation accompany the dramatic changes in the absorption properties that are induced by DMS reduction.

Vibrational Modes of Bound DMSO. The close correspondence in the resonance Raman spectra and excitation profiles of the Mo−S and dithiolene vibrational modes in DMS- and dithionite-reduced samples indicates that both are des-oxo-Mo(IV) forms of the enzyme with identical dithiolene and serinate Mo coordination. However, the visible absorption

(23) Koehler, B. P.; Mukund, S.; Conover, R. C.; Dhawan, I. K.; Roy, R.; Adams, M. W. W.; Johnson, M. K. *J. Am. Chem. Soc.* **1996**, *118*, 12391−12405.

(24) Nakamoto, K. *Infrared and Raman spectra of inorganic and coordination compounds*; John Wiley & Sons: New York, 1986.

(25) Collin, R. J.; Griffith, W. P.; Pawson, D. *J. Mol. Struct.* **1973**, *19*, 531−544.

spectrum of DMS-reduced DMSO reductase shows an intense charge transfer transition centered near 550 nm that is not present in dithionite-reduced samples (Figure 7), and excitation into this band results in maximal enhancement of two additional Raman bands at 497 and 862 cm^{-1} (Figures 6 and 7). Moreover, when the DMSO-reoxidized sample is utilized in which only the Mo═O unit is labeled with ^{18}O, both of these modes were shown to involve vibrations of this bound oxygen. The 497 cm^{-1} band has an 18 cm^{-1} ^{18}O downshift, and the 862 cm^{-1} band has a 29 cm^{-1} ^{18}O downshift (Figure 6). The magnitude of the ^{18}O shift of the 862 cm^{-1} band in the DMS-reduced sample distinguishes this mode from the Mo═O stretching mode in the Mo(VI) sample which also occurs at 862 cm^{-1}. The absence of any Mo(VI) form in this sample is further demonstrated by the lack of the intense Mo−S stretching band at 350 cm^{-1} that dominates the spectrum of the as-prepared Mo(VI) form with 530 and 568 nm excitation (Figure 3). On the basis of the frequencies and isotope shifts, the 497 and 862 cm^{-1} bands in DMS-reduced DMSO reductase are assigned to the Mo−O and S═O stretching modes of bound DMSO. A simple diatomic oscillator calculation predicts ^{18}O downshifts of 25 and 33 cm^{-1} for Mo−O and S═O vibrations, respectively. The slightly smaller observed shifts are expected as a result of the larger effective mass of the bridging O atom and, in the case of the Mo−O mode, kinematic coupling with Mo-S vibrations. The Mo−O stretching frequency is indicative of a Mo-O single bond, and the S═O stretching frequency is greatly reduced from that in free DMSO (ν(S═O) = 1003 cm^{-1}) suggesting a bond order of approximately 1.5. These results provide the first direct evidence that the oxo group on Mo(VI) is the site of attack by DMS and suggest that the 550 nm absorption band corresponds to a Mo(IV)-to-DMSO charge transfer band.

The marked similarity in the resonance Raman spectra of dithionite- and DMS-reduced samples is clearly best interpreted in terms of replacement of a coordinated water molecule by bound DMSO with minimal perturbation of the other Mo ligands. However, we have been unable to obtain any direct evidence for a coordinated water molecule in dithionite-reduced samples. A Mo−OH_2 stretching mode should be readily identified by an ^{18}O downshift of approximately 20 cm^{-1} for samples exchanged into $H_2{}^{18}O$ buffer, but none of the bands observed in 300−600 cm^{-1} region of the spectrum of dithionite-reduced Mo(IV) obtained with 568 nm excitation (Figure 5a) were sensitive to $H_2{}^{18}O/H_2{}^{16}O$ buffer exchange. In contrast, the bands centered at 461 and 589 cm^{-1} in the spectrum obtained with 488 nm excitation (Figure 5b) shifted down by 13 and 11 cm^{-1}, respectively, for samples prepared in $H_2{}^{18}O$ buffer. However, control experiments with dithionite-treated $H_2{}^{18}O$ and $H_2{}^{16}O$ buffer solutions identified these bands as spontaneous Raman bands arising from excess dithionite. They are more apparent at this wavelength due to the decreased enhancement of the dithiolene or pyran ring deformations and Mo−S-(dithiolene) stretching modes with 488 nm excitation.

Discussion

The resonance Raman results presented above provide unambiguous evidence that *R. sphaeroides* DMSO reductase is catalytically competent for direct oxygen atom transfer with the active-site cycling between mono-oxo-Mo(VI) and des-oxo-Mo-(IV) forms and suggest that both molybdopterin dithiolenes remain firmly attached to Mo at all stages of the catalytic cycle. Moreover, the ability to selectively label and monitor the bound oxo group affords unique insight into the catalytic mechanism and the nature of the substrate-bound intermediate. Structures based on the resonance Raman data for each of the four forms

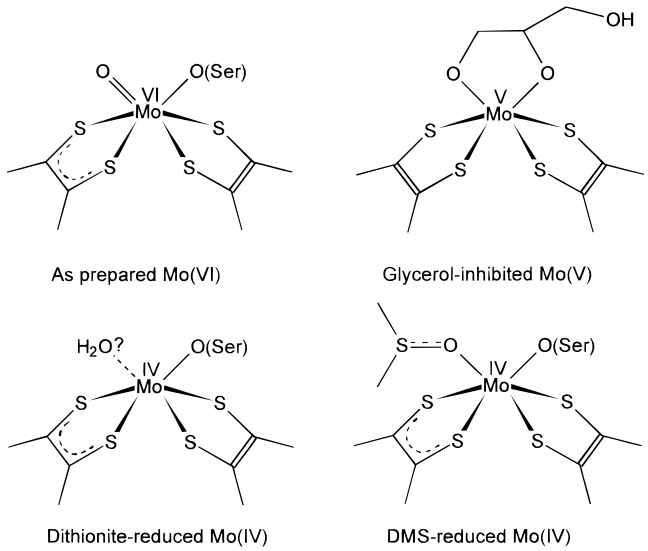

Figure 11. Resonance-Raman-derived active-site structures for the DMSO reductase derivatives investigated in this work. The dithiolenes in the glycerol-inhibited Mo(V) form are both depicted as dithiolate-type. On the basis of the observed ν(C═C) stretching frequencies (1550 and 1567 cm^{-1}, unpublished observations), both are likely to be intermediate between the π-delocalized- and dithiolate-type dithiolenes that are present in the other three derivatives. However, this assignment should be viewed as tentative and awaits detailed studies of the high-frequency region of this derivative with isotopically labeled diols.

of DMSO reductase investigated in this work are presented in Figure 11. The approximate trigonal prismatic coordination geometry derives from the crystallographic data for the Mo-(VI) form of the *R. sphaeroides* enzyme,[3] and the only evidence for the coordinated water molecule shown in the dithionite-reduced Mo(IV) form comes from the Mo-EXAFS studies of this enzyme.[7] Other than this, the Mo coordination environments for the structures shown in Figure 11 have been deduced from the resonance Raman data. These structures define four out of the five species in the reaction scheme shown in Figure 12, and the resonance Raman evidence for each is summarized below in the context of this catalytic cycle.

The complete analyses of the resonance Raman spectra of the as-prepared Mo(VI), dithionite-reduced Mo(IV), and DMS-reduced Mo(IV) forms of *R. sphaeroides* DMSO reductase in the 200−1700 cm^{-1} region and the glycerol-inhibited Mo(V) form in the 200−550 cm^{-1} region show that *all* of the observed bands can be accounted for in terms of vibrational modes involving atoms in the Mo first or second coordination sphere or the chelating dithiolenes. In particular, there is no longer any need to invoke conjugation of the dithiolene C═C with a pterin C═C of a 5,8-dihydro form of molybdopterin to explain the appearance of the two strong bands at 1527 and 1578 cm^{-1} in the Mo(VI) form or coupling of Mo−S with molybdopterin modes to rationalize the ^{34}S shifts in the Mo−S stretching region.[14] These proposals were made prior to the discovery that the Mo is coordinated by two molybdopterin dithiolenes[3,15] and the crystallographic evidence that the both molybdopterins are at the tetrahydro oxidation level in Mo(VI) and Mo(IV) states.[3] It is now evident, based on the data presented herein, that the bands at 1527 and 1572−1578 cm^{-1} arise from the C═C stretching modes of two distinct types of dithiolene and that the Mo−S stretching modes can be reassigned in terms of vibrational modes of a square pyramidal MoS_4 unit.

Taken together, the resonance Raman evidence for four Mo−S vibrations in as-prepared Mo(VI), glycerol-inhibited Mo-(V), dithionite-reduced Mo(IV), and DMS-reduced Mo(IV)

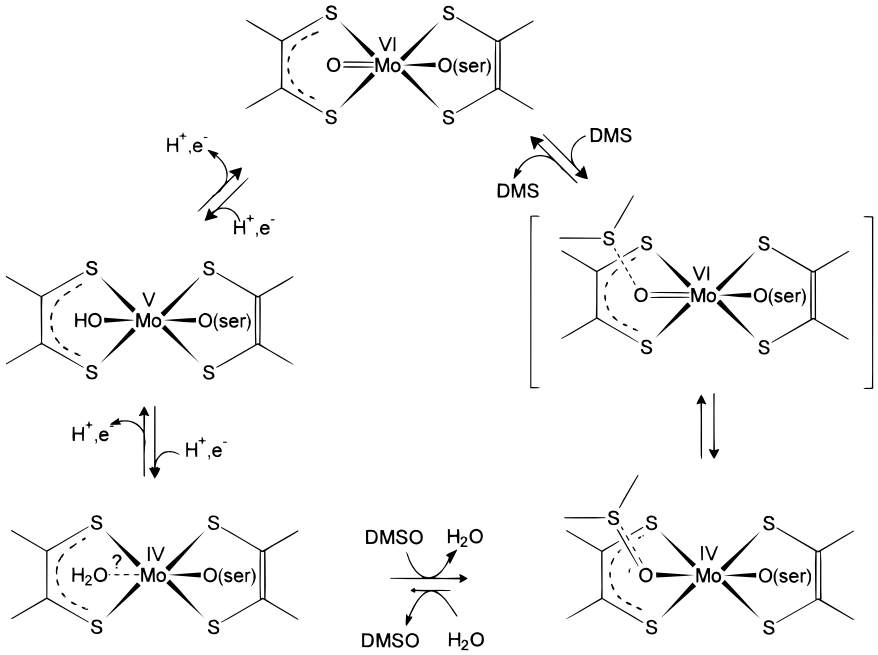

Figure 12. Proposed catalytic cycle for DMSO reductase.

forms and two sets of dithiolene modes in the as-prepared Mo(VI), dithionite-reduced Mo(IV), and DMS-reduced Mo(IV) forms provide convincing evidence that both types of dithiolene remain coordinated as bidentate chelating ligands during catalytic turnover. This is in contrast to the crystallographic results obtained with dithionite-soaked crystals, which showed dissociation of one of the molybdopterin dithiolene ligands.[3] The resonance Raman data indicate that dithionite or DMS reduction in solution occurs with an overall shortening of the Mo—S bonds as evidenced by the increase in the average Mo—S stretching frequency (358 cm^{-1} for Mo(VI), 362 cm^{-1} for Mo(V), and 375 cm^{-1} for Mo(IV)). This is in qualitative agreement with Mo-EXAFS data which indicate average Mo—S distances of 2.44 Å in as-prepared Mo(VI) (∼4 Mo—S bonds), 2.40 Å in glycerol-inhibited Mo(V) (∼4 Mo—S bonds), and 2.33 Å in dithionite-reduced Mo(IV) (3−4 Mo—S bonds). However, according to Badger's rule,[26] a shortening of 0.11 Å in the Mo—S bond length should translate to a 57-cm^{-1} increase in the vibrational frequency, more than three times the observed average Mo—S frequency shift on going from Mo(VI) to Mo(IV) (17 cm^{-1}). The origin of this discrepancy is unclear at present, but we suspect that it reflects different Mo—S distances for each type of dithiolene ligand.

Resonance Raman analyses of dithiolene vibrational modes in dithiolene-coordinated oxo-Mo complexes have largely been confined to identifying one Mo—S stretching frequency and the C═C stretching mode.[27,28] Intense C═C stretching modes have been reported at 1472 and 1491 cm^{-1} for $[Mo^{VI}O_2(S_2C_2(CN)_2)_2]^{2-}$ and $[Mo^{IV}O(S_2C_2(CN)_2)_2]^{2-}$, respectively,[28] and at 1503 and 1535 cm^{-1} for $[Mo^{VI}O_2(S_2C_2(COOMe)_2)_2]^{2-}$ and $[Mo^{IV}O(S_2C_2(COOMe)_2)_2]^{2-}$, respectively.[27,28] For the former pair of complexes, resonance Raman spectra were reported over the 100−1700 cm^{-1} region and vibrational modes that are candidates for the ν(C-C), ν(C-C) + ν(C-S) and ν(C-S) + ν(C-C) modes were observed in the 1000−1200 cm^{-1} region but not assigned.[28] Given these results for model compounds, the absence of major frequency shifts in the dithiolate-type or π-delocalized-type dithiolene stretching frequencies in DMSO reductase as a function of the Mo oxidation state is surprising. Only the dithiolate-type dithiolene shows an appreciable shift on going from Mo(VI) to Mo(IV), but in contrast to the model systems, the shift in the ν(C═C) frequencies is only 6 cm^{-1} and opposite in sign, i.e., larger frequency for Mo(VI). In light of the evidence that oxo groups have a strong *trans* influence,[29] this behavior suggests that the π-delocalized-type dithiolene is *trans* to the serinate which remains attached in both oxidation states, whereas the dithiolate-type dithiolene is *trans* to the oxo group which is lost on reduction. The loss of the oxo group would be compensated for by increased Mo—S π-bonding in the dithiolate-type dithiolene thereby increasing the Mo—S bond strength (shorter Mo—S bonds) and resulting in greater π-delocalization in the dithiolene ring and hence a lower ν(C═C) frequency in the Mo(IV) state. This arrangement of the two types of dithiolene in relation to the oxo and serinate ligands in the Mo(VI) state (see Figure 11) leads to the conclusion that it is the dithiolate-type dithiolene that can be partially or fully dissociated under the crystallization conditions[3,4] (see Figure 2). Hence, the π-delocalized-type and dithiolate-type dithiolenes are provisionally assigned to molybdopterin P and Q, respectively, in terms of the labeling used in the X-ray structures.[3,4]

The identification of two types of coordinated dithiolene in DMSO reductase has important consequences for interpreting the excited state electronic properties of mononuclear Mo and W enzymes. Excitation profiles for the dithiolene and Mo—S modes in DMSO reductase and human sulfite oxidase,[16] which has only the π-delocalized-type dithiolene, clearly demonstrate that the dithiolate-type dithiolene is responsible for the low-energy (>500 nm) electronic transitions. Hence the 640 nm absorption band in dithionite-reduced Mo(IV),[8a] the 720 nm absorption band in as-prepared Mo(VI),[8a] and the low-energy (>500 nm) absorption and VTMCD bands of the glycerol-inhibited Mo(V) form[11] are all assigned to thiolate-to-Mo charge transfer bands. These electronic transitions are particularly effective for enhancing Mo—S stretching modes of both types of dithiolene. In the case of the π-delocalized dithiolene, it

(26) Herschbach, D. R.; Laurie, V. W. *J. Chem. Phys.* **1961**, *35*, 458−463.

(27) Subramanian, P.; Burgmayer, S.; Richards, S.; Szalai, V.; Spiro, T. G. *Inorg. Chem.* **1990**, *29*, 3849−3853.

(28) Oku, H.; Ueyama, N.; Nakamura, A. *Inorg. Chem.* **1995**, 3667−3676.

(29) Ueyama, N.; Oku, H.; Kondo, M.; Okamura, T.; Yoshinaga, N.; Nakamura, A. *Inorg. Chem.* **1996**, *35*, 643−650.

seems likely that the enhancement of Mo—S stretching modes occurs via kinematic coupling, since negligible resonance enhancement of these modes occurs in human sulfite oxidase even at wavelengths <500 nm when the dithiolene modes are maximally enhanced.[16] For this reason, the higher energy electronic transitions associated with the π-delocalized dithiolene are probably best considered as π-dithiolene-to-Mo charge transfer. The presence of a π-delocalized-type dithiolene in other single molybdopterin enzymes would also explain the very weak VTMCD spectrum of glycerol-inhibited Mo(V) form of desulfo xanthine oxidase[30] and account for the negligible resonance enhancement of Mo—S(dithiolene) stretching modes in Raman spectra of milk xanthine oxidase[31] and *Desulfovibrio gigas* aldehyde oxidoreductase.[32] While a detailed discussion of the excited state electronic structure of Mo(V) and W(V) centers in enzymes and model complexes will be published elsewhere, it is clear that a dithiolate-type dithiolene is a prerequisite for the low-energy charge transfer bands and intense VTMCD spectra that are only observed in enzymes with bis-molybdopterin dithiolene coordination.

In addition to the molybdopterin dithiolenes ligands, the available resonance Raman, EXAFS,[7] and crystallographic[3,4] data all indicate that Ser147 is coordinated as a serinate in all forms of enzyme, except the diol-inhibited Mo(V) derivatives. Weak bands at 536 cm^{-1} (Mo(VI)) and 513 cm^{-1} (Mo(IV) forms) are assigned to Mo—O(Ser) stretching on the basis of sensitivity to Mo oxidation state, insensitivity to $H_2{}^{18}O$ buffer exchange, and loss of bands in this region on formation of the diol-inhibited Mo(V) form. The diol-inhibited Mo(V) derivative is an oxygen-insensitive stable form of the enzyme that is trapped in the Mo(V) state by addition of 50% (v/v) glycerol or ethylene glycol after one-electron reduction of the as-prepared Mo(VI) form using reduced benzyl viologen. EXAFS,[7] EPR,[11] and VTMCD[11,23] data indicate that the stability of this inhibited form results from a tris-chelate structure in which serinate and hydroxide ligands are replaced by a chelating diol. The EPR evidence is particularly convincing, since the principal *g*-values are identical to the Mo(V) species seen in redox titration of the active enzyme, in accord with identical first shell coordination environment for the Mo(V) centers, and the only difference resides in loss of the proton splitting from the coordinated hydroxide.[11] Hence, this derivative can be viewed as a stable analog for the Mo(V) species in the catalytic cycle shown in Figure 12.

Catalytic activity of DMSO reductase is therefore primarily associated with the sixth coordination position on Mo, and resonance Raman provides a direct method for monitoring ligation at this site. Evidence for a mono-oxo-Mo(VI) species comes from the single Mo═O stretching at 862 cm^{-1} in as-prepared Mo(VI) samples. The 43 cm^{-1} ^{18}O isotope shift both confirms this conclusion and shows that the mono-oxo form is catalytically competent for direct oxygen atom transfer, since the oxo group could be labeled either by reoxidation of the dithionite-reduced Mo(IV) sample after exchange into $H_2{}^{18}O$ buffer (left side of catalytic scheme in Figure 12) or by reoxidation with $DMS^{18}O$ in $H_2{}^{16}O$ buffer (right side of catalytic scheme in Figure 12). The absence of the 862 cm^{-1} band in the dithionite-reduced Mo(IV) form is in accord with a des-oxo formulation, but the question of whether the sixth coordination site is vacant or occupied by a weakly coordinated water molecule, as suggested by Mo-EXAFS studies,[7] still remains to be determined. No evidence for a coordinated water molecule was apparent in the crystal structure of dithionite-reduced *R. sphaeroides* DMSO reductase,[3] and despite extensive $H_2{}^{18}O$ labeling studies, none has been forthcoming from resonance Raman.

Direct evidence for the DMSO-bound Mo(IV) intermediate species shown in Figure 11 comes from resonance Raman of the DMS-reduced sample (Figure 6). The ability to selectively label the bound oxo group in the Mo(VI) samples with ^{18}O by reoxidation of dithionite-reduced samples with $DMS^{18}O$ facilitates identification of the S═O and Mo—O stretching modes of bound DMSO in the DMS-reduced sample via isotope shifts and provides direct evidence that the oxo group on Mo(IV) is the site of product attack. The Mo—O stretch of bound DMSO occurs at 497 cm^{-1} and is characteristic of a single bond. DMSO binding to a transition metal ion through oxygen invariably results in decrease of the S═O stretching frequency (1003 cm^{-1} in free DMSO), and this is readily understood in terms of the relative contributions of the two resonance hybrid structures:

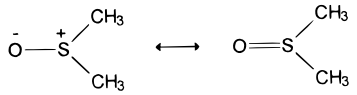

However, the S═O stretching frequency of bound DMSO in DMSO reductase, 862 cm^{-1}, is substantially lower than those found in oxygen-coordinated transition metal ion complexes (910−960 cm^{-1} for Mn(II), Fe(II,III), Ni(II), Cu(II), Zn(II), and Cd(II)[24]) indicating a much greater weakening of the S═O double bond. This is clearly consistent with the role of the Mo-(IV) in binding and activating the substrate for S—O bond cleavage. The partial positive charge on the S atom of the bound DMSO accounts for the low-energy Mo(IV)-to-S charge transfer transition that gives rise to the cherry red color of the DMS-reduced enzyme and provides the mechanism for resonance enhancement of the Mo—O and S═O stretching modes.

The resonance Raman deduced structures shown in Figure 11 and the ability to interconvert between these forms while monitoring the nature, origin, and fate of the oxygen ligand at the six coordination position lead to the mechanistic scheme shown in Figure 12. In essence this mechanism confirms the oxygen atom transfer hypothesis proposed by Schultz et al.[17] but demonstrates that the catalytic cycle involves mono-oxo and des-oxo states rather than di-oxo and mono-oxo states. In addition, the present study provides a more complete description of the Mo coordination environment at each stage of the catalytic cycle. It differs from the scheme proposed on the basis of the crystallographic studies of as-prepared Mo(VI) and dithionite-reduced Mo(IV) forms of *R. sphaeroides* DMSO reductase,[3] in that the Mo remains six coordinate with all four sulfurs of the molybdopterin dithiolene ligands firmly attached throughout the catalytic cycle. Starting from the mono-oxo-Mo(VI) form, catalysis proceeds by two sequential one-electron/one-proton additions, with the electrons coming from an exogenous electron donor, to yield the des-oxo-Mo(IV) form, via an hydroxide-ligated Mo(V) intermediate. The putative weakly-bound water molecule is then displaced by DMSO which is bound exclusively through the oxygen with concomitant weakening of the S═O bond. The stability of this substrate-bound intermediate is demonstrated by the limited extent of the reverse reaction in DMS-reduced samples. The electron withdrawing ability of the *trans* dithiolene ligand to form the more localized dithiolate-type dithiolene that is observed in the Mo(VI) form is likely to play the key role in driving the reformation of the mono-oxo-Mo(VI) species and liberation of the product, DMS. Hence,

(30) Peterson, J.; Godfrey, C.; Thomson, A. J.; George, G. N.; Bray, R. C. *Biochem. J.* **1986**, *233*, 107−110.
(31) Oertling, W. A.; Hille, R. *J. Biol. Chem.* **1990**, *265*, 17446−17450.
(32) Zhelyaskov, V.; Yue, K. T.; LeGall, J.; Barata, B. A. S.; Moura, J. J. G. *Biochim. Biophys. Acta* **1995**, *1252*, 300−304.
(33) Centeno, J. A. *Arch. Biochem. Biophys.* **1992**, *292*, 624−628.

the dithiolate-type dithiolene ligand is proposed to play a crucial electronic role in the catalytic mechanism. The role of the π-delocalized-type dithiolene ligand that is common to both DMSO reductase and sulfite oxidase is less obvious. In addition to anchoring the Mo to the protein, this molybdopterin could provide the conduit for electron transfer to or form the Mo site and/or poising the Mo(IV)/Mo(V) and Mo(V)/Mo(VI) midpoint potentials at the appropriate level for the reaction at hand. It will clearly be of interest to establish the type of molybdopterin dithiolene ligands in other enzymes of this general class.

At present there is no resonance Raman or EXAFS evidence for the existence of the di-oxo-Mo(VI) form of DMSO reductase with a dissociated molybdopterin dithiolene, as seen in the crystal structure of the *R. capsulatus* enzyme (see Figure 2).[4] Nevertheless, in light of the EPR evidence for a Mo(V) species analogous to that found in desulfo xanthine oxidase, under certain conditions of dithionite reduction,[6] it seems probable that such a species can exist. We have shown here that the mono-oxo-Mo(VI)/des-oxo-Mo(IV) form of DMSO reductase is catalytically competent for DMSO reduction via an oxygen atom transfer mechanism. However, at this stage we cannot exclude the possibility that a di-oxo-Mo(VI)/mono-oxo-Mo(IV) form of DMSO reductase is also catalytically competent via a similar or different mechanism. Further experiments to define more precisely the conditions required for active site interconversions, and the catalytic activity in each state are planned to address this important issue.

While the potential of resonance Raman spectroscopy for investigating the catalytic mechanisms, active-site structures, and electronic properties of mononuclear Mo/W enzymes has long been recognized, the results reported here for DMSO reductase represent the first example where this potential has been fully exploited. This approach will be more difficult in enzymes containing additional prosthetic groups, but the vibrational assignments presented here set the stage for major advances in the use of resonance Raman for investigating the Mo or W active sites of other enzymes, particularly those in which the only other type of chromophoric species are Fe−S clusters. Both the spectroscopic and crystallographic data for DMSO reductase attest to the plasticity of the Mo coordination environment, and it is apparent that the active-site structure is critically dependent on crystallization conditions and/or medium effects. A combination of both spectroscopic and crystallographic approaches is therefore required to reach reliable conclusions about the molecular mechanism of catalysis in Mo and W oxotransferases and hydroxylases. Moreover, since resonance Raman and EXAFS can be used with crystalline and solution samples in the diamagnetic Mo/W(VI) or Mo/W(IV) oxidation states, one or both of these techniques should be used to assess the possibility of active-site structural changes induced by crystallization.

Acknowledgment. This work was supported by grants from the NSF (MCB9419019 to M.K.J.), the NIH (GM00091 to K.V.R.), and by a NSF Research Training Group Award to the Center for Metalloenzyme Studies (DBI-9413236).

Note Added in Proof. An alternative proposal for the catalytic cycle of DMSO reductase has recently been published (Baugh, P. E.; Garner, C. D.; Charnock, J. M.; Collison, D.; Davies, E. S.; McAlpine, A. S.; Bailey, S.; Lane, I.; Hanson, G. R.; McEwan, A. G. *JBIC, J. Biol. Inorg. Chem.* **1997**, *2*, 634−643). X-ray crystallographic and Mo-EXAFS studies of oxidized and DMS-reduced forms of *R. capsulatus* DMSO reductase have been interpreted in terms of a seven-coordinate Mo site in both oxidation states: four S ligands from the two molybdopterins bound via their dithiolene groups, one O ligand from serine, one short "spectator" oxo (Mo−O, 1.7 Å), and one long oxo group (Mo−O, 1.9 Å) that is hydrogen bonded to a tryptophan in the MO(VI) state and attached to DMS in the DMS-reduced form. The catalytic cycle was therefore proposed to involve only the long terminal oxo group which is poised for oxygen atom transfer. This proposal is not consistent with the resonance Raman presented herein for *R. sphaeroides* DMSO reductase. In addition to the absence of any evidence for a spectator oxo group, the vibrational frequency of the *substrate and solvent exchangeable* Mo═O group can only be interpreted in terms of a short terminal oxo group (i.e., ∼1.7 Å), as opposed to a long terminal oxo group (i.e., ∼1.9 Å).

JA972109L